Jurnal Polimesin
Department of Mechanical Engineering
State Polytechnic of Lhokseumawe
http://e-jurnal.pnl.ac.id/polimesin
e-ISSN : 2549-1999 No. : 2 Month : April
p-ISSN : 1693-5462 Volume : 24 Year : 2026

Processing dates: received on 2025-9-24, reviewed on 2026-03-03, accepted on 2026-03-19 and online availability on 2026-04-25

# Performance and efficiency analysis of a 1600 Wp PV system: investigation of thermal, system configuration, and exergy aspects

**Suwarti[1,*], Yusuf Dewantoro Herlambang[1], F. Gatot Sumarno[1], Margana[1], Baktiyar Mei Hermawan[1], Zya Jamaluddin Al Rasyid[1], Wisnu Dyka Pradana[1], Robiatul Muztaba[2]**

[1]Mechanical Engineering, Politeknik Negeri Semarang, Semarang 50275, Indonesia

[2]Atmospheric and Palnetary Science, Institut Teknologi Sumatera, South Lampung 35365, Indonesia

*Coresponding author: suwarti0707@gmail.com

**Abstract**

A hybrid photovoltaic system with a total installed capacity of 1.6 kWp, composed of monocrystalline and polycrystalline modules, was experimentally evaluated under tropical conditions. The energy storage system employs a 72V bank comprising lithium-ion and lead-acid batteries. Hourly experimental measurements were conducted, and exergy analysis based on the Second Law of Thermodynamics was applied to quantify irreversible losses. It is revealed that the system's energy efficiency ranges from 3.33% to 8.67%. The peak efficiency occurred in the afternoon, coinciding with lower panel temperatures and greater direct power delivery. Quantitative exergy analysis further identified a maximum exergy destruction of 8486.88 W at the irradiance peak, with the lowest exergetic efficiency dropping to 3.61% due to thermal irreversibilities. Additionally, operational monitoring revealed a critical synchronization failure between the lithium Battery Management System (BMS) and the Solar Charge Controller (SCC) during low-voltage states, necessitating manual intervention for recovery. These findings highlight that thermal management and component synchronization are the primary bottlenecks for system reliability in tropical environments.

**Keywords:**

Solar power plant, solar panel efficiency, exergy, bottleneck.

## 1 Introduction

The demand for electrical energy in Indonesia continues to increase in line with population growth, urbanization, and technological developments. However, the national electricity supply is still dominated by fossil fuel power plants, such as coal, petroleum, and natural gas, which contribute significantly to greenhouse gas emissions and environmental pollution. This situation calls for a transition to cleaner and more sustainable renewable energy sources [1], [2].

Among renewable energy sources, solar energy offers substantial potential in Indonesia due to its equatorial location. The mean daily solar radiation intensity in Indonesia varies from 4.5 to 5.0 kWh/m²/day, corresponding to an estimated national solar potential of approximately 207.8 GWp [3], [4]. Despite this abundance, the installed solar capacity remains limited at about 0.085 GWp, accounting for only 0.04% of the total potential. Photovoltaic (PV) technology enables direct conversion of solar radiation into electrical energy and is suitable for both residential and commercial applications [5].

The implementation of a solar power plant in the field encounters several technical challenges, such as variations in efficiency due to changes in radiation intensity, elevated panel temperatures, suboptimal installation orientation, and limited battery energy storage capacity. These factors influence system performance and the quality of the generated energy [6]. The potential of solar energy is also hindered by a critical limitation: the relatively low efficiency of solar cells. Efficiency is variable and is substantially affected by changes in current-voltage (I–V) and power-voltage (P–V) characteristics. Moreover, parameters such as open-circuit voltage (Voc), short-circuit current (I–sc), and fill factor exhibit sensitivity to variations in temperature [7], [8]. Consequently, a comprehensive technical analysis is required to assess the real-world performance of solar power plants and to identify the influencing factors [6], [9].

It is essential to bear in mind that solar panel manufacturers typically conduct measurements in laboratories under Standard Test Conditions (STC) of 25°C, 1000 W/m², and Air Mass (AM) of 1.5. In reality, each region and climatic condition deviates significantly from STC, leading to efficiency results that may differ from the manufacturer's catalog specifications. Some research evaluates photovoltaic efficiency or performance under actual conditions. Each photovoltaic panel or module has a distinct efficiency rating, and a 1°C rise in temperature can affect photovoltaic efficiency, either positively or negatively, depending on the specific type of panel [10]. The selection of module technology must be considered, as it may be affected by the environment in which it is used [11].

A multitude of investigations have scrutinized PV performance analysis, including one investigation [12], [13] that assessed electrical performance, exergy components, and exergy efficiency in solar panels, and another by [14], [15], [16] that evaluated PV performance features from an exergy standpoint. The previously referenced research [12] indicated that the evaporative cooling method can lower the temperature of solar panels by up to 22.3% and increase output power by 73%, a finding further validated by exergy analysis.

Another research study [15], [16] has also conducted energy and exergy analysis on photovoltaic systems, finding that exergy productivity decreases with increasing temperature. Other research [17] performed simulations using PVsyst software and conducted an outdoor experiment, revealing that a 1°C rise in temperature led to a 0.07% increase in current and a 0.34% decrease in voltage. The power generated diminished to 0.49%, while efficiency fell to 0.59%.

Investigations have been conducted to develop methods to lower the operating temperature of solar photovoltaic panels. A study [18] investigated the effectiveness of various passive and active cooling methods in enhancing solar panel efficiency. Another example is [19], which employs airflow to enhance convection for the thermal regulation of solar panels. The outcome was a 12% improvement in efficiency. A separate study [20] indicates that the efficiency of solar photovoltaic systems can improve by 35% when operating under cooler conditions with the implementation of a cooling system. A separate investigation [21] indicates that using fins to enhance efficiency can yield a 22.24% improvement over conventional bare cells in a floating PV system.

Several researchers [21], [22], [23] have also conducted studies on installing PV modules on water surfaces, which are naturally cooled by the microclimate in which they operate, thereby reducing thermal power losses and improving energy performance. This also has several advantages, such as minimal land use and reduced evaporation in water reservoirs.

While these studies provide valuable insights, most existing literature focuses on large-scale solar farms or conventional residential PV systems, often assuming uniform battery chemistry and idealized energy storage behavior. There remains a notable lack of experimental research addressing thermodynamic bottlenecks in medium-capacity PV systems (≈1.6 kWp) dedicated to lighting

applications in tropical urban environments. Furthermore, empirical investigations into hybrid energy storage configurations combining lithium-ion and lead-acid batteries—particularly regarding operational synchronization with Solar Charge Controllers (SCC)—are still scarce.

Therefore, this study experimentally investigates a 1.6 kWp off-grid photovoltaic system installed in Jabungan Village, Semarang City, Indonesia. The research focuses on two main aspects: (1) system configuration and operational behavior, including hybrid battery storage performance, and (2) thermodynamic evaluation using energy and exergy analysis to identify dominant sources of efficiency degradation. Special attention is given to thermal accumulation effects and system-level reliability issues arising from the lack of synchronization between the Battery Management System (BMS) and SCC. The findings aim to provide practical and thermodynamically grounded insights for improving the performance and reliability of photovoltaic systems operating in tropical climates.

## 2 Research methodology

### 2.1 System description

The research was conducted in Jabungan Village, Banyumanik District, Semarang City, Indonesia, and focused on the experimental evaluation of an off-grid PV power generation system used exclusively for lighting applications under tropical environmental conditions. The investigated system has a total installed PV capacity of 1.6 kWp.

The photovoltaic array employs a hybrid configuration consisting of both monocrystalline and polycrystalline modules, with a combined surface area of 10.92 m². The array consists of two 200 Wp monocrystalline modules, four 100 Wp monocrystalline modules, six 100 Wp polycrystalline modules, and four 50 Wp polycrystalline modules, resulting in equal contributions of 800 Wp from monocrystalline panels and 800 Wp from polycrystalline panels. All PV modules are mounted on a fixed supporting structure with an optimized tilt angle to maximize daily solar irradiance capture under local climatic conditions.

The balance of system (BOS) components include six SCCs—two rated at 100 A and four at 50 A—which regulate power flow from the PV array to the energy storage system and protect the batteries from overcharging and deep discharge under fluctuating irradiance conditions.

A distinctive feature of the investigated system is the implementation of a dual-chemistry energy storage configuration, combining a lithium-ion battery bank and a lead-acid battery bank, operating at a nominal DC bus voltage of 72 V. Lithium-ion batteries offer high energy density and fast dynamic response. In contrast, lead-acid batteries provide operational robustness and cost-effectiveness. Both battery banks are configured through series–parallel arrangements to match the system voltage.

During system operation, it was observed that the lithium-ion battery bank is protected by an internal BMS that operates independently from the SCCs. Under low battery conditions, the BMS disconnects the lithium-ion battery from the electrical circuit to prevent deep discharge and cell degradation. Consequently, when photovoltaic charging power becomes available, the incoming energy cannot be directly delivered to the battery once the BMS protection is activated. This lack of synchronization between the BMS and the SCC results in a complete system shutdown, even in the presence of sufficient solar irradiance. This operational characteristic represents a critical system-level constraint in hybrid photovoltaic energy storage systems.

A DC–AC inverter converts the stored DC electrical energy into AC power for the lighting load. At the same time, an Automatic Transfer Switch (ATS) ensures safe and reliable operation. Electrical output is monitored using a kWh meter installed on the AC side of the system. All analyses presented in this study are conducted at the system level, using the 72 V DC bus as the reference operating condition.

### 2.2 Experimental procedure

A field-based experimental approach was employed to evaluate the operational performance of the photovoltaic system under real tropical environmental conditions. Data acquisition was conducted over five consecutive days, from July 22 to July 26, 2025, during daytime operation.

Prior to the measurements, all monitoring instruments—including a solar power meter and a digital multimeter—were calibrated to ensure measurement accuracy and data reliability. Visual inspections were performed at the beginning of each measurement day to confirm proper system operation, unobstructed solar exposure, and the absence of shading on the photovoltaic modules.

Measurements commenced at 09:00 (UTC+7) and were subsequently recorded at one-hour intervals until 15:00 (UTC+7). At each measurement interval, key operating parameters were recorded simultaneously to ensure data consistency. These parameters included solar irradiance (G), output voltage (V), and output current (I) of the photovoltaic system. Ambient temperature data were also logged to support thermodynamic and exergy analysis.

The selected measurement window corresponds to the dominant daily solar exposure period and captures the variation in system performance under changing irradiance and thermal conditions. The collected dataset was then used as the basis for subsequent evaluations of energy and exergy performance.

### 2.3 Data analysis and performance calculation

The system's performance was evaluated by calculating the input power, output power, and overall efficiency using the measured field data. The explicit use of the equations is for calculating the system's performance metrics.

#### 2.3.1 Energy analysis (first law of thermodynamics)

The fundamental performance metrics based on the First Law of Thermodynamics, which quantifies the energy flow, were calculated using the measured field data: (1) the calculation of solar panel input power ($P_{in}$) is performed using the Eq. (1), where G is the solar irradiance, and A is the surface area of the solar panel; (2) the solar panel output power ($P_{out}$) was calculated using the Eq. (2), where $V_{out}$ and $I_{out}$ are the measured output voltage and current from the solar panel, respectively; (3) finally, the system efficiency ($\eta$) is determined using the ratio of the output power to the input power, as formulated in Eq. (3).

$$P_{in} = G \times A \tag{1}$$

$$P_{out} = V_{out} \times I_{out} \tag{2}$$

$$\eta = \frac{P_{out}}{P_{in}} \times 100\% \tag{3}$$

#### 2.3.2 Exergy analysis (second law of thermodynamics)

An exergy analysis was also conducted to evaluate the quality of the electrical energy produced relative to the available radiation energy. This analysis quantifies the irreversible thermodynamic losses. All temperatures are expressed in Kelvin (K).

Critical parameters and assumptions: (1) solar temperature ($T_{sun}$), based on standard thermodynamic literature for PV analysis, the sun's surface temperature was set at 5777°K; (2) ambient temperature ($T_{ambient}$), based on the data log, the ambient temperature was confirmed to be almost constant at 31°C (304.15°K) during the 11:00 a.m. to 3:00 p.m. testing window.

Exergy calculation metrics: (1) input exergy ($Ex_{in}$), the exergy rate of incident solar radiation is calculated by multiplying the input power by the radiation exergy factor or Petela limit factor, as given in Eq. (4). This formulation is derived from Petela's model and accounts for the thermodynamic quality of solar radiation; (2) electrical energy is considered pure exergy, the output exergy is

equal to the electrical output power (Eq. (5)); (3) the exergetic efficiency of the PV system is defined as Eq. (6); the exergy destruction represents irreversible losses occurring within the system and is calculated as Eq. (7).

$$E_{x,in} = P_{in}\left[1 - \frac{4}{3}\left(\frac{T_{ambient}}{T_{sun}}\right) + \frac{1}{3}\left(\frac{T_{ambient}}{T_{sun}}\right)^4\right] \quad (4)$$

$$E_{x,out} = P_{out} \quad (5)$$

$$\eta_{ex} = \frac{E_{x,out}}{E_{x,in}} \times 100\% \quad (6)$$

$$I_{ex} = E_{x,in} - E_{x,out} \quad (7)$$

The results from both analyses were used to identify daily efficiency trends and the influencing factors from both system configuration and exergy/energy perspectives. The analysis accounted for energy conversion losses resulting from elevated panel temperatures, the SCC-imposed limitations on battery charging, and inverter conversion losses. The results were analyzed to identify daily efficiency trends and the influencing factors from both the system configuration perspective and the exergy/energy perspective.

## 3 Results and discussion

### 3.1 System testing

Testing of the 1600 Wp solar power system in Jabungan Village was conducted over five days, from July 22 to 26, 2025, with hourly data recorded between 09:00 a.m. and 3:00 p.m (Fig. 1 and Fig. 2). Measured parameters included solar irradiance (G), panel output voltage (V), panel output current (I), and battery charging conditions (Table 1).

Solar radiation intensity generally increased from morning, peaked between 12:00 noon and 1:00 p.m., and declined in the afternoon. Conventionally, peak electrical efficiency is expected to coincide with peak irradiance. However, the data reveal a critical divergence: maximum efficiency was typically observed in the afternoon, despite lower radiation intensity. This suggests that, as irradiance peaks, increased thermal loading can actually decrease the PV module's electrical efficiency, resulting in higher efficiency later in the day when the module temperature is lower, even as irradiance declines. This demonstrates how the PV module's thermal behavior significantly influences the final electrical output.

Fig. 1. Realization of solar power generation for lighting loads.

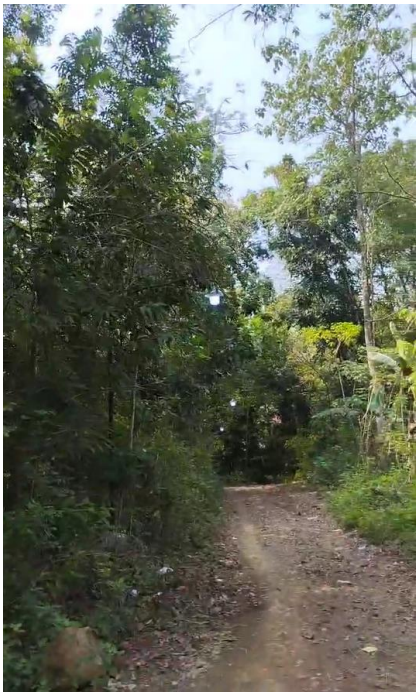

Fig. 2. Lamp load for solar power generation.

Table 1. Test data for Tuesday, July 22, 2025

| Time (UTC +7) | Specified load (Watt) | From solar panel (DC) | | From inverter (AC) | | Solar irradiance (W/m²) | Cos Phi | Output power (Watt) or $V_{out} \times I_{out}$ | Input power (Watt) or $G \times A$ | Efficiency (%) |
|---|---|---|---|---|---|---|---|---|---|---|
| | | Voltage (Volt) | Current (Amp.) | Output voltage (Volt) | Output current (Amp.) | | | | | |
| 09:00 | 40 | 108.29 | 3.02 | 229 | 0.155 | 607.35 | 0.95 | 327.0358 | 6632.262 | 4.93% |
| | 140 | | | 229 | 0.521 | | 0.99 | | | |
| | 240 | | | 229 | 0.885 | | 0.99 | | | |
| 10:00 | 40 | 106.5 | 3.15 | 230 | 0.158 | 802.31 | 0.95 | 335.4775 | 8761.225 | 3.83% |
| | 140 | | | 229 | 0.533 | | 0.99 | | | |
| | 240 | | | 229 | 0.896 | | 0.99 | | | |
| 11:00 | 40 | 107.7 | 3.38 | 229 | 0.158 | 849.69 | 0.95 | 361.998 | 9278.615 | 3.90% |
| | 140 | | | 229 | 0.535 | | 0.99 | | | |
| | 240 | | | 230 | 0.897 | | 0.99 | | | |
| 12:00 | 40 | 106.9 | 2.98 | 230 | 0.16 | 867.05 | 0.95 | 318.562 | 9468.186 | 3.36% |
| | 140 | | | 228 | 0.526 | | 0.99 | | | |
| | 240 | | | 230 | 0.892 | | 0.99 | | | |
| 13:00 | 40 | 111.7 | 2.62 | 229 | 0.146 | 804.19 | 0.95 | 292.654 | 8781.755 | 3.33% |
| | 140 | | | 229 | 0.515 | | 0.99 | | | |
| | 240 | | | 228 | 0.877 | | 0.99 | | | |
| 14:00 | 40 | 100.7 | 2.57 | 231 | 0.147 | 679.15 | 0.95 | 258.799 | 7416.318 | 3.49% |
| | 140 | | | 229 | 0.502 | | 0.99 | | | |
| | 240 | | | 228 | 0.9 | | 0.99 | | | |
| 15:00 | 40 | 107.1 | 2.88 | 229 | 0.149 | 517.23 | 0.95 | 308.448 | 5648.152 | 5.46% |
| | 140 | | | 228 | 0.531 | | 0.99 | | | |
| | 240 | | | 227 | 0.908 | | 0.99 | | | |

To visualize the impact of thermal conditions on performance, Fig. 3 combines the profiles of solar irradiance, ambient temperature, and system efficiency. The graph reveals a distinct 'crossing pattern' that highlights the thermal bottleneck.

As shown in Fig. 3, solar irradiance (bars) and ambient temperature (red line) rise in parallel, peaking at 12:00 p.m. (867.05 W/m² and 31°C). Conversely, the system efficiency (green line) moves in the opposite direction, dropping to its lowest point (3.36%) at the same time. Although the measured temperature represents the ambient condition ($T_{amb}$), the PV modules' operating temperature is thermodynamically estimated to be significantly higher due to solar absorption. This visual evidence confirms that high solar availability paradoxically leads to a decrease in conversion efficiency due to thermal saturation. To quantify the exact energy quality lost due to this heat, a detailed exergy analysis is presented in Table 3 (Section 3.3).

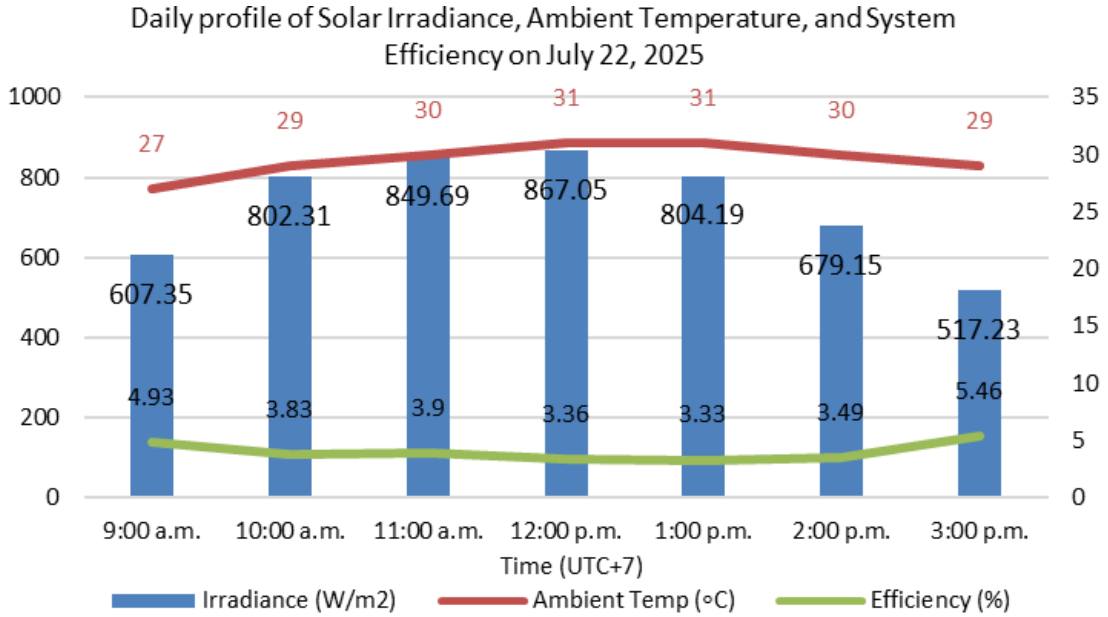


Fig. 3. Daily profile of solar irradiance, ambient temperature, and system efficiency on July 22, 2025.

In contrast, the highest efficiency that day, 5.46%, was recorded at 3:00 p.m., when irradiance had fallen significantly to 517.3 W/m². This outcome demonstrates that, even with reduced sunlight, lower afternoon panel temperatures effectively reduce thermal losses and increase the module's operating voltage, thereby improving efficiency. Continuous exposure to high midday irradiance causes the panel's surface temperature to accumulate and peak later, usually between 12:00 p.m. and 1:00 p.m.—precisely when efficiency begins its steepest decline.

Consequently, the findings make clear that panel temperature control, rather than solar irradiance alone, governs the daily efficiency patterns of the PV system in this equatorial climate. This highlights a fundamental challenge in PV operation where the thermodynamic quality of the energy conversion is degraded by heat, a concept explored further in the exergy analysis (Section 3.3).

Additionally, the lowest efficiency of 3.33% was recorded at 1 p.m., coinciding with high panel temperatures and restricted charging current from the SCC as the battery neared full capacity.

Fig. 3 (July 22) visualizes the inverse relationship between temperature and efficiency. As shown, the efficiency dropped to 3.36% at the peak temperature. This thermal degradation pattern was consistent across all observed days; including July 23, confirming that the phenomenon is systematic and not an anomaly (see Table 2). The highest efficiency of 8.67% occurred at 3:00 p.m., while the lowest, 3.92%, occurred at 10:00 a.m.

Table 2. Test data for Tuesday, July 23, 2025

| Time (UTC +7) | Specified load (Watt) | From solar panel (DC) | | From inverter (AC) | | Solar irradiance (W/m²) | Cos Phi | Output power (Watt) or $V_{out} \times I_{out}$ | Input power (Watt) or $G \times A$ | Efficiency (%) |
|---|---|---|---|---|---|---|---|---|---|---|
| | | Voltage (Volt) | Current (Amp.) | Output voltage (Volt) | Output current (Amp.) | | | | | |
| 09:00 | 40 | 106 | 3.03 | 227 | 0.16 | 720.68 | 0.95 | 321.18 | 7869.826 | 4.08% |
| | 140 | | | 227 | 0.512 | | 0.99 | | | |
| | 240 | | | 227 | 0.906 | | 0.99 | | | |
| 10:00 | 40 | 108 | 3.11 | 228 | 0.156 | 784.52 | 0.95 | 335.88 | 8566.958 | 3.92% |
| | 140 | | | 230 | 0.522 | | 0.99 | | | |
| | 240 | | | 229 | 0.894 | | 0.99 | | | |
| 11:00 | 40 | 125.9 | 3.31 | 229 | 0.15 | 845.6 | 0.95 | 416.729 | 9233.952 | 4.51% |
| | 140 | | | 229 | 0.512 | | 0.99 | | | |
| | 240 | | | 227 | 0.905 | | 0.99 | | | |
| 12:00 | 40 | 143.1 | 3.6 | 229 | 0.151 | 860.26 | 0.95 | 515.16 | 9394.039 | 4.58% |
| | 140 | | | 230 | 0.518 | | 0.99 | | | |
| | 240 | | | 229 | 0.904 | | 0.99 | | | |
| 13:00 | 40 | 129.1 | 3.88 | 230 | 0.151 | 806.18 | 0.95 | 500.908 | 8803.486 | 5.69% |
| | 140 | | | 230 | 0.512 | | 0.99 | | | |
| | 240 | | | 229 | 0.907 | | 0.99 | | | |
| 14:00 | 40 | 114.1 | 3.73 | 230 | 0.15 | 663.5 | 0.95 | 425.593 | 7245.42 | 5.87% |
| | 140 | | | 230 | 0.519 | | 0.99 | | | |
| | 240 | | | 230 | 0.905 | | 0.99 | | | |
| 15:00 | 40 | 107.2 | 4.48 | 230 | 0.153 | 507.36 | 0.95 | 480.256 | 5540.371 | 8.67% |
| | 140 | | | 228 | 0.513 | | 0.99 | | | |
| | 240 | | | 230 | 0.898 | | 0.99 | | | |

Conclusion of daily patterns: this repeated pattern, confirmed across all five days of the experimental period, confirms that lower panel temperatures in the afternoon consistently yield higher system efficiency than periods of peak radiation. The influence of the SCC on system throttling, as evidenced by the voltage suppression on July 23, will be explored further in Section 3.2, and the thermodynamic implications of thermal losses will be discussed in Section 3.3.

### 3.2 From the system configuration perspective

The operational performance of the photovoltaic system is analyzed from a system configuration perspective, treating the 1.6 kWp PV installation as an integrated energy conversion system. In this framework, solar irradiance serves as the primary energy resource, while the electrical power delivered to the load constitutes the useful output. The system employs a hybrid photovoltaic array consisting of monocrystalline modules, which exhibit superior performance under high irradiance conditions, and polycrystalline modules, which provide relatively stable output under low to moderate irradiance levels.

Key system components include the SCCs, a DC–AC inverter for power conversion, and an ATS. The SCCs regulate power flow from the photovoltaic array to the energy storage system and protect the batteries from overcharging and excessive discharge. The energy storage subsystem consists of a dual-chemistry configuration combining lithium-ion and lead-acid battery banks operating at a nominal DC bus voltage of 72 V.

Building on this system overview, the analysis reveals that constraints imposed by the SCC play a central role in the observed efficiency anomalies. Two distinct operational behaviors were identified, corresponding to hard and soft SCC constraints. A hard constraint was observed on July 23 at 10:00 (UTC+7), when the system recorded its lowest efficiency (3.92%). During this period, the PV array output voltage dropped sharply to 108 V (Table 2), indicating an active intervention by the SCC. This behavior suggests that the SCC temporarily deprioritized Maximum Power Point Tracking (MPPT) in favor of rapid bulk charging, likely in response to a low battery State of Charge (SOC).

The release of this hard constraint was confirmed at 11:00 (UTC+7), when the panel voltage abruptly increased to 125.9 V, indicating a return to MPPT operation. In contrast, a soft constraint was observed on July 22 at 12:00 (UTC+7), coinciding with peak solar irradiance. Despite high irradiance levels, the panel voltage remained nearly constant at approximately 115.1 V (Table 1), and system efficiency dropped to 3.36%. This behavior indicates gradual current limitation by the SCC, driven by elevated panel temperatures and a near-full battery condition. Under these circumstances, the SCC shifted the operating point away from the maximum power point, resulting in reduced electrical output despite abundant solar input. Table 2 shows the battery voltage fluctuations during the observation. A crucial finding in this study is the identification of a safety cutoff threshold of 21.7V, set by the battery's BMS. When the voltage reached this 21.7V limit, the BMS automatically disconnected the power to prevent deep discharge, causing a system shutdown even though solar irradiance was still available.

Taken together, these observations highlight the SCC as a critical operational bottleneck within the system. This bottleneck is further compounded by the lack of synchronization between the SCC and the lithium-ion BMS. When the BMS activates low-voltage protection, it disconnects the lithium-ion battery bank from the system, preventing immediate charging even when solar input becomes available. Complementing this behavior, the ATS ensures load continuity by switching to the utility grid during periods of low photovoltaic output. While this strategy maintains power availability, it reduces the effective utilization of renewable energy. Collectively, these interacting constraints define the system's dominant performance limitations and reinforce the importance of coordinated control and thermal management in hybrid photovoltaic systems operating in tropical environments.

### 3.3 From the exergy perspective

In addition to conventional electrical performance indicators, an exergy-based analysis grounded in the Second Law of Thermodynamics was employed to evaluate the quality of energy conversion within the photovoltaic system. While electrical output power reflects the amount of energy produced, exergy analysis provides a quantitative measure of energy degradation due to thermodynamic irreversibilities, particularly those associated with thermal effects.

The experimental findings in Section 3.1 established that thermal accumulation, rather than irradiance, governs the daily efficiency pattern. This decline in electrical efficiency is strongly correlated with a rise in the panel's surface temperature ($T_p$). As $T_p$ increases, the panel's open-circuit voltage ($V_{oc}$) decreases, hich directly reduces the electrical power output of the photovoltaic module. This thermal behavior directly influences the quality of energy conversion and is therefore critical from a Second Law perspective.

As presented in Table 3, the exergy destruction ($I_{ex}$) exhibits a strong dependence on solar irradiance. At 09:00 (UTC+7), with an ambient temperature of 27°C and a solar irradiance of 607.35 W/m$^2$. The calculated exergy destruction was 5845.52 W. As solar irradiance increased toward midday, $I_{ex}$ rose significantly, reaching a maximum value of 8486.88 W at 12:00 (UTC+7), corresponding to a peak irradiance of 867.05 W/m$^2$.

The observed increase in exergy destruction at higher irradiance levels indicates that although the available solar exergy input increases, a substantial portion of this energy is irreversibly degraded due to enhanced thermal effects. Consequently, higher solar availability does not necessarily translate into improved exergetic performance under conditions of insufficient thermal dissipation.

The exergetic efficiency ($\eta_{ex}$) reached its minimum value of 3.61% at midday, despite the maximum incident solar power. This behavior confirms that elevated panel temperatures intensify entropy generation, thereby reducing the fraction of useful work that can be extracted from the incoming solar radiation. From a Second Law standpoint, the simultaneous occurrence of maximum irradiance and minimum exergetic efficiency highlights the dominant role of thermal irreversibilities in limiting system performance.

Table 3. Quantitative exergy analysis results on Tuesday, July 22, 2025

| Time (UTC+7) | Tamb (°C) | Irradiance (G) (W/m$^2$) | Input exergy (Ex,in) (W) | Output power (Pout) (W) | Exergy destruction (Iex) (W) | ηex (%) |
|---|---|---|---|---|---|---|
| 09:00 | 27 | 607.35 | 6172.55 | 327.03 | 5845.52 | 5.29% |
| 10:00 | 29 | 802.31 | 8148.15 | 335.47 | 7812.68 | 4.11% |
| 11:00 | 30 | 849.69 | 8625.12 | 361.99 | 8263.13 | 4.19% |
| 12:00 | 31 | 867.05 | 8805.44 | 318.56 | 8486.88 | 3.61% |
| 13:00 | 31 | 804.19 | 8167.03 | 292.65 | 7874.38 | 3.58% |
| 14:00 | 30 | 679.15 | 6893.92 | 258.79 | 6635.13 | 3.75% |
| 15:00 | 29 | 517.23 | 5251.72 | 308.44 | 4943.28 | 5.87% |

Beyond thermal effects, system-level operational constraints further exacerbate exergy losses. In particular, the lack of synchronization between the lithium-ion BMS and the SCCs leads to additional exergy destruction. Under low battery conditions, the BMS disconnects the battery from the electrical circuit to prevent deep discharge. As a result, incoming solar power cannot be utilized to recharge the battery once this protection mode is activated; forcing the system into a shutdown state even when solar input is available.

Overall, these results demonstrate that although the photovoltaic system effectively intercepts solar radiation, the energy conversion process is constrained by a dominant thermodynamic bottleneck. This bottleneck arises from the combined effects of thermal accumulation on the photovoltaic modules and system-level operational constraints, particularly the lack of synchronization between the BMS and the SCCs. Under such conditions, a significant portion of the available solar exergy cannot be converted into useful electrical work, even at high irradiance levels. Consequently, performance degradation in tropical photovoltaic systems is governed not by solar resource availability but by irreversible losses associated with thermal effects and protection-driven system interruptions. Addressing this thermodynamic bottleneck through effective thermal management and coordinated control strategies is therefore essential for enhancing exergetic performance and overall system reliability.

## 4 Conclusions

This study concludes that the 1600 Wp PV system for lighting achieves a peak energy efficiency of 8.67%, yet faces significant thermodynamic limitations. Quantitative exergy analysis identifies a peak exergy destruction of 8486.88 W during mid-day, proving that thermal irreversibility is the primary cause of energy quality degradation in tropical climates. Moreover, the integration of a hybrid lithium and lead-acid storage bank reveals a critical synchronization gap; the lithium BMS cutoff at 21.7 V prevents autonomous system recovery. Future improvements must prioritize active panel cooling and enhanced SCC-BMS communication protocols to maximize both energy quality and system reliability.

## References


[1] L. Kanugrahan and E. Sujarwanto, "Komparasi Potensi Bahan Panel Surya Berdasarkan Iklim Kota Tasikmalaya," *DIFFRACTION*, vol. 3, no. 2, pp. 62–67, Jul. 2022, doi: 10.37058/diffraction.v3i2.5379.

[2] J. Windarta, Denis, A. Firmansyah, A. I. Avinda, and I. A. Kusuma, "Technical study of 1.2 KWP solar plant on Tanbihul Ghofilin Islamic Boarding School Banjarnegara," *IOP Conf Ser Earth Environ Sci*, vol. 969, no. 1, p. 012031, Jan. 2022, doi: 10.1088/1755-1315/969/1/012031.

[3] E. Yusuf, Jakariya, and A. Subeno, "Planning for the Development of a 40 kWp Off-Grid Centralized Solar Power Plant (SPP) on Insumbabi Island," *Jurnal Konversi Energi dan Manufaktur*, Jul. 2025, doi: 10.21009/JKEM.10.2.4.

[4] Suryati, S. H. Pambudi, J. L. Wibowo, and N. I. Partiwi, *Outlok Energi Indonesia*. Sekretaris Jenderal Dewan Energi Nasional, 2019.

[5] S. Utami and A. Daud, "Pengaruh Temperatur Panel Surya terhadap Efisiensi Panel Surya Sistem Monitoring menggunakan Internet of Things (IoT)," *Energi*, vol. 10, no. 1, pp. 7–10, 2020, doi: https://doi.org/10.35313/.v11i1.2437.

[6] N. Kapilan, K. C. Nithin, and K. N. Chiranth, "Challenges and opportunities in solar photovoltaic system," *Mater Today Proc*, vol. 62, pp. 3538–3543, Jan. 2022, doi: 10.1016/j.matpr.2022.04.390.

[7] M. S. Khan, V. Hegde, and G. Shankar, "Effect of Temperature on Performance of Solar Panels- Analysis," in *2017 International Conference on Current Trends in Computer, Electrical, Electronics and Communication (CTCEEC)*, IEEE, Sep. 2017, pp. 109–113. doi: 10.1109/CTCEEC.2017.8455109.

[8] N. Milind, M. Antony, F. Francis, J. Francis, J. Varghese, and S. U K, "Enhancing the Efficiency of Solar Panel Using Cooling Systems," *Int J Eng Res Appl*, vol. 07, no. 03, pp. 05–07, Mar. 2017, doi: 10.9790/9622-0703040507.

[9] R. Rahayu, "Peningkatan Arus Listrik Dan Tegangan Listrik Keluaran Sel Surya Dengan Menggunakan Reflektor," *Simetris*, vol. 16, no. 2, pp. 49–52, 2022, doi: 10.51901/simetris.v16i2.269.

[10] E. Elibol, Ö. T. Özmen, N. Tutkun, and O. Köysal, "Outdoor performance analysis of different PV panel types," *Renewable and Sustainable Energy Reviews*, vol. 67, pp. 651–661, Jan. 2017, doi: 10.1016/j.rser.2016.09.051.

[11] C. Ma, R. Wu, Z. Liu, and X. Li, "Performance assessment of different photovoltaic module technologies in floating photovoltaic power plants under waters environment," *Renew energy*, vol. 222, p. 119890, Feb. 2024, doi: 10.1016/j.renene.2023.119890.

[12] M. Alktranee and B. Péter, "Energy and exergy analysis for photovoltaic modules cooled by evaporative cooling techniques," *Energy Reports*, vol. 9, pp. 122–132, Dec. 2023, doi: 10.1016/j.egyr.2022.11.177.

[13] K. Guedri, M. Salem, M. E. H. Assad, J. Rungamornrat, F. Malek Mohsen, and Y. M. Buswig, "PV/Thermal as Promising Technologies in Buildings: A Comprehensive Review on Exergy Analysis," *Sustainability*, vol. 14, no. 19, p. 12298, Sep. 2022, doi: 10.3390/su141912298.

[14] S. Sukumaran and K. Sudhakar, "Performance analysis of solar powered airport based on energy and exergy analysis," *Energy*, vol. 149, pp. 1000–1009, Apr. 2018, doi: 10.1016/j.energy.2018.02.095.

[15] A. R. Hakim, W. T. Handoyo, and P. Wullandari, "An energy and exergy analysis of photovoltaic system in Bantul Regency, Indonesia," *Journal of Mechatronics, Electrical Power, and Vehicular Technology*, vol. 9, no. 1, pp. 1–7, Jul. 2018, doi: 10.14203/j.mev.2018.v9.1-7.

[16] Kandukuri Kumari and D. Chandra Sekhar, "Energy and Exergy Analysis of Solar PV System," *International Transactions on Electrical Engineering and Computer Science*, vol. 1, no. 2, pp. 62–67, Dec. 2022, doi: 10.62760/iteecs.1.2.2022.24.

[17] M. K. Al-Ghezi, R. T. Ahmed, and M. T. Chaichan, "The Influence of Temperature and Irradiance on Performance of the photovoltaic panel in the Middle of Iraq," *International Journal of Renewable Energy Development*, vol. 11, no. 2, pp. 501–513, May 2022, doi: 10.14710/ijred.2022.43713.

[18] Filip Grubišić-Čabo, Sandro Nižetić, and Tina Giuseppe Marco, "Photovoltaic panels: A Review of the Cooling Techniques," *TRANSACTIONS OF FAMENA XL - Special issue 1 (2016)*, no. 1, 2016.

[19] A. Kasaeian, Y. Khanjari, S. Golzari, O. Mahian, and S. Wongwises, "Effects of forced convection on the performance of a photovoltaic thermal system: An experimental study," *Exp Therm Fluid Sci*, vol. 85, pp. 13–21, Jul. 2017, doi: 10.1016/j.expthermflusci.2017.02.012.

[20] Z. Peng, M. R. Herfatmanesh, and Y. Liu, "Cooled solar PV panels for output energy efficiency optimisation," *Energy Convers Manag*, vol. 150, pp. 949–955, Oct. 2017, doi: 10.1016/j.enconman.2017.07.007.

[21] N. A. S. Elminshawy, D. G. El-Damhogi, I. A. Ibrahim, A. Elminshawy, and A. Osama, "Assessment of floating photovoltaic productivity with fins-assisted passive cooling," *Appl Energy*, vol. 325, p. 119810, Nov. 2022, doi: 10.1016/j.apenergy.2022.119810.

[22] G. M. Tina, F. Bontempo Scavo, L. Merlo, and F. Bizzarri, "Analysis of water environment on the performances of

floating photovoltaic plants," *Renew Energy*, vol. 175, pp. 281–295, Sep. 2021, doi: 10.1016/j.renene.2021.04.082.
[23] M. Dörenkämper, A. Wahed, A. Kumar, M. de Jong, J. Kroon, and T. Reindl, "The cooling effect of floating PV in two different climate zones: A comparison of field test data from the Netherlands and Singapore," *Solar Energy*, vol. 219, pp. 15–23, May 2021, doi: 10.1016/j.solener.2021.03.051.